Int. J. Heat Mass Transfer. Vol. 8, pp. 67–82. Pergamon Press 1965. Printed in Great Britain

STUDY ON FORCED CONVECTIVE HEAT TRANSFER IN CURVED PIPES

(*1ST REPORT, LAMINAR REGION*)

YASUO MORI and WATARU NAKAYAMA

Department of Mechanical Engineering, Tokyo Institute of Technology, Tokyo, Japan

(*Received* 22 *June* 1964)

Abstract—The theoretical study of fully developed laminar flow in a curved pipe gives a satisfactory result for resistance coefficient and heat-transfer coefficient in fully developed temperature field under the condition of uniform heat flux at large Dean numbers [$= Re\sqrt{(a/R)}$]. The ratio of the Nusselt number for a curved pipe flow to that for a straight pipe flow is obtained as a function of Dean number and Prandtl number. As Dean number and Prandtl number increase, the effect of curvature on flow resistance and heat transfer increases, but the Nusselt number ratio approaches to the asymptotic value with the increasing Prandtl number. Experimental study is carried out for air flow in a curved pipe. The velocity and temperature distributions are measured and the Nusselt number ratio obtained by the experiments is shown to be in good agreement with that of the theoretical analysis.

NOMENCLATURE

A, w_1 at the centre of a cross section perpendicular to the pipe axis;
A', g_1 at the centre of a cross section perpendicular to the pipe axis;
a, radius of the pipe;
C, coefficient, $\equiv -(\partial P/H\,\partial\theta)$;
c_p, specific heat of fluid at constant pressure;
D, intensity of the secondary flow in the flow core;
$f_{\theta r}, f_{\theta\psi}$, tangential stresses in the direction of pipe axis;
G, $\equiv T_w - T$;
g, $\equiv G/\tau a$;
K, Dean number, $\equiv Re\sqrt{(a/R)}$;
k, heat conductvity of fluid;
Nu, Nusselt number, $\equiv [2aq/k(T_w - T_m)]$;
P, $\equiv (a^2/\nu^2)\,(p/\rho)$;
Pr, Prandtl number, $\equiv \rho c_p \nu/k$;
p, pressure;
q, heat flux at the wall to the fluid per unit area and unit time;
q_η, q_ψ, dimensionless transferred heat in the fluid;
R, radius of curvature of the pipe axis;
Re, Reynolds number, $\equiv (2aW_m/\nu)$;
r, co-ordinate in radial direction in the cross section;
T, temperature;
T_m, mixed mean fluid temperature;
T_w, wall temperature;
U, radial component of velocity, $u \equiv Ua/\nu$;
V, circumferential component of velocity, $v \equiv Va/\nu$;
W, axial component of velocity, $w \equiv Wa/\nu$;
W_m, mean velocity, $w_m \equiv W_m a/\nu$;
x_i, horizontal co-ordinate of a mesh of the cross section, when the axis of the curved pipe is placed in a horizontal plane;
y_j, vertical co-ordinate of a mesh.

Greek symbols

δa, thickness of the velocity boundary layer;
$\delta_t a$, thickness of the thermal boundary layer;
ζ, thickness ratio, $\equiv \delta_t/\delta$;
H $\equiv R/a$;
η, $\equiv r/a$;
θ, axial co-ordinate;
λ, resistance coefficient,

$$\equiv \left(-\frac{\partial p}{R\,\partial\theta}\right)\frac{2a}{\frac{1}{2}\rho W_m^2};$$

μ, viscosity;

ν, $\equiv \mu/\rho$;
ξ, $\equiv 1 - \eta$;
ρ, density;
$\tau_{\theta\eta}$, $\equiv \left(\frac{a^2}{\nu^2}\right)\left(\frac{f_{\theta r}}{\rho}\right)$; $\tau_{\theta\psi} \equiv \left(\frac{a^2}{\nu^2}\right)\left(\frac{f_{\theta\psi}}{\rho}\right)$;
τ, temperature gradient along the pipe axis;
ψ, circumferential co-ordinate.

Suffixes

0, value at the pipe wall;
1, value in the flow core region;
I, first approximation;
II, second approximation;
m, mean value taken around the periphery ($\psi = 0 \sim 2\pi$);
δ, value at the edge of the velocity boundary layer;
δ_t, value at the edge of the thermal boundary layer.

INTRODUCTION

HEAT TRANSFER in a curved pipe is of fundamental importance in various heat exchangers having heating or cooling coils. Curved pipes are also used for heat transfer in heat engines and industrial equipment. However, only few papers have been reported for this problem, in particular no theoretical analysis is known.

The first experimental study was done by Jeschke [1] for turbulent flow of air. His empirical formula was revised by Merkel [2] and the revised formula is found as Jeschke's formula in many books. Hawes [3] tried to investigate velocity and temperature distributions in a curved pipe flow, but the data on the temperature field were not certain ones. Ede [4] suggested from his experimental results a method to calculate the heat-transfer coefficient for a right-angled bend. Recently Seban and McLaughlin [5] presented experimental data on heat transfer for laminar flow of oil and turbulent flow of water in curved pipes.

Experimental studies of flow resistance in a curved pipe have been done by investigators. The data on the resistance coefficient are well summarized by Ito [6]. On the other hand, a satisfactory explanation of the flow field has not yet been given theoretically. The first theoretical study was done by Dean [7] for fully developed laminar flow. Using a perturbation method he tried to find deviation of a velocity profile from the Poiseuille flow pattern by solving the Navier–Stokes equations. He pointed out that a secondary flow is set up and the dynamical similarity introduces a parameter $K = Re\sqrt{a/R}$ which is called Dean number. However, his solution is applicable only in quite small Dean number regions, and his formula for the resistance coefficient is not useful enough for practical use. Adler [8] closely examined the velocity distributions by experiment, and found that a velocity profile of laminar flow differs greatly from the parabolic distribution. Hence he discussed the fully developed laminar flow assuming a thin boundary layer along the wall. His formula for the resistance coefficient asymptotically approaches to the observed results in very large Dean numbers. The same assumption of boundary layer is employed by Barua [9] for the analysis of laminar flow and by Ito [6] for turbulent flow. However, as shown later in the arguments by these authors there is incompleteness, and no theoretical approach to the problem of heat transfer has been done so far.

The purpose of this paper is to give a precise investigation on heat-transfer rate in a curved pipe for fully developed laminar flow under the condition of uniform heat flux, over a fairly wide range of Dean number. Physical properties are regarded as constant. The first part of this paper is devoted to a theoretical study of flow field, in which incompleteness in the previous theories is excluded. In the second part, the temperature field is discussed. In the latter part experiments were made for air flow in a uniformly heated curved pipe of radius ratio 40. Velocity and temperature distributions in the pipe were measured by means of a one-hole yaw probe and a thermocouple probe. From the observed distributions, mixed mean temperatures were computed and Nusselt numbers were calculated to compare with those obtained by theoretical analysis.

THEORETICAL ANALYSIS OF THE FLOW IN A CURVED PIPE

In a curved pipe the fluid in the central part is driven toward the outer wall by centrifugal force. The fluid near the wall flows along the wall

surface to the inner wall as shown in Fig. 7. Thus in the pipe the secondary flow forms a couple of vortices in a cross section of the pipe. In order to investigate the effect by the secondary flow in the flow field, balance of forces in the direction of the pipe axis is considered at first. Forces are viscous stress, stress caused by the secondary flow of the fluid and pressure force. For a steady and fully developed laminar flow, pressure gradient along the pipe axis is constant. When the system of co-ordinates is taken as shown in Fig. 1 and $r/R \ll 1$ is assumed, the force balance equation is expressed in the following non-dimensional form;

$$\frac{\partial}{\eta\,\partial\eta}(\eta\tau_{\theta\eta}) + \frac{\partial\tau_{\theta\psi}}{\eta\,\partial\psi} = -C\,(\text{constant}) \quad (1.1)$$

where the tangential stresses are (see Fig. 1)

$$\left.\begin{aligned}\tau_{\theta\eta} &\equiv \frac{a^2}{\nu^2}\cdot\frac{f_{\theta r}}{\rho} = \frac{\partial w}{\partial\eta} - uw \\ \tau_{\theta\psi} &\equiv \frac{a^2}{\nu^2}\cdot\frac{f_{\theta\psi}}{\rho} = \frac{\partial w}{\eta\,\partial\psi} - vw\end{aligned}\right\} \quad (1.2)$$

Analogous to Reynolds stress in turbulent flow, uw and vw are stresses caused by the secondary flow and predominate over an entire cross section of the pipe except the narrow layer near the wall surface in large Dean number regions. These tangential stresses may be supposed to introduce the additional pressure loss to a flow in a curved pipe.

Hereafter, the region where viscous stress might be ignored is called a core region of the flow, and in this region the velocity components u, v, w, are denoted by u_1, v_1, w_1. On the other hand the region adjacent to the wall is called a boundary layer.

1. *The velocity distributions in the core region*

The tangential stresses in the core region are expressed by

$$\tau_{\theta\eta} = -u_1 w_1, \quad \tau_{\theta\psi} = -v_1 w_1 \quad (1.3)$$

The curvilinear motion of fluid produces pressure distribution across the pipe section. The relations between the centrifugal force and the pressure gradients in the cross section are

$$\frac{w_1^2}{H}\cos\psi = \frac{\partial P}{\partial\eta}, \quad \frac{w_1^2}{H}\sin\psi = -\frac{\partial P}{\eta\,\partial\psi} \quad (1.4)$$

Elimination of the pressure terms from these equations yields the following relation for the axial velocity component in the core region

$$\cos\psi\frac{\partial w_1}{\eta\,\partial\psi} + \sin\psi\frac{\partial w_1}{\partial\eta} = 0 \quad (1.5)$$

From this equation and the equation of continuity $[\partial(\eta u_1)/\eta\,\partial\eta] + (\partial v_1/\eta\,\partial\psi) = 0$ the following special solution is obtained and will be shown to be reasonable by experimental analysis

$$\left.\begin{aligned}u_1 &= D\cos\psi \\ v_1 &= -D\sin\psi \\ w_1 &= A + \frac{C}{D}\eta\cos\psi\end{aligned}\right\} \quad (1.6)$$

where A and D are constants.

Therefore the secondary flow in the core region is seen to be expressed by a uniform flow toward the outer wall. Of course, the actual flow field is

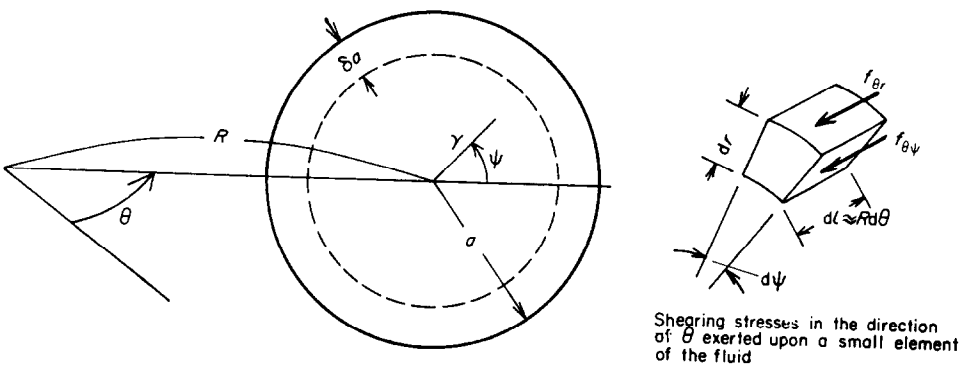

FIG. 1. System of co-ordinates.

more complicated and the compensation will be introduced in the later analysis.

2. *The velocity distributions in the boundary layer*

According to the relations of (1.6), the fluid in the core region flows toward the outer wall, and then enters the thin layer close to the wall and is pushed back along the wall toward the inner side by the pressure gradient. In consideration of the flow field in the cross section shown in Fig. 2, the flow rate of the secondary flow through the plane *B–O* is to be equal to that

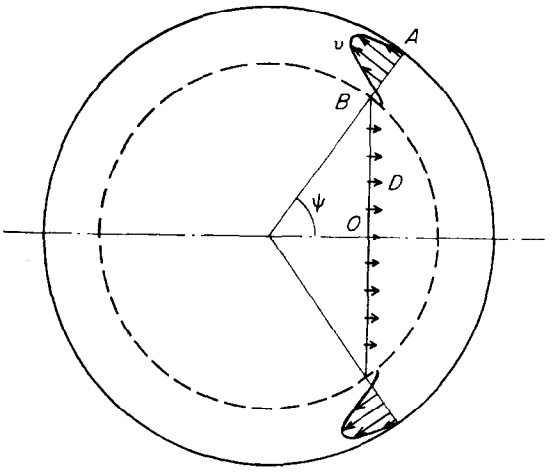

FIG. 2. Continuity of the secondary flow rate.

through the plane *A–B*. If δ is taken as the thickness of the boundary layer, the equation of continuity is written as

$$\int_0^{\delta} v \, d\xi = D(1 - \delta) \sin\psi \qquad (1.7)$$

The velocity components v, w in the boundary layer can be determined from equation (1.7) and the following boundary conditions:

at $\xi = 0$ $\quad v = w = 0$

at $\xi = \delta$ $\quad v = v_1, \quad \dfrac{\partial v}{\partial \xi} = 0,$

$$w = w_{1\delta}, \quad \frac{\partial w}{\partial \xi} = -\left(\frac{\partial w_1}{\partial \eta}\right)_{\delta}$$

So as to satisfy the conditions shown above the velocity components are expressed as,

$$\left.\begin{aligned} v &= -D \sin\psi \left[\left(-\frac{12}{\delta} + 6\right)\frac{\xi}{\delta} + \left(\frac{24}{\delta} - 9\right)\frac{\xi^2}{\delta^2} + \left(-\frac{12}{\delta} + 4\right)\frac{\xi^3}{\delta^3}\right] \\ w &= w_{1\delta}\left(2\frac{\xi}{\delta} - \frac{\xi^2}{\delta^2}\right) + \frac{\delta C}{D}\cos\psi\left(\frac{\xi}{\delta} - \frac{\xi^2}{\delta^2}\right) \end{aligned}\right\} \qquad (1.8)$$

In the previous analytical works by Adler and Barua, etc., some of the boundary conditions cited above are not satisfied at the edge of the boundary layer, the velocity profile is not joined smoothly to that in the core region and v does not vanish at $\psi = \pi$. By putting v as that in equation (1.8) this unreasonableness can be omitted. Examples of the velocity distributions in the boundary layer are shown in Fig. 3.

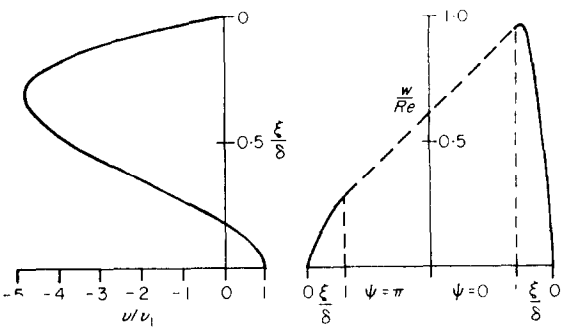

FIG. 3. Velocity distributions in the boundary layer (when $\delta = 0{\cdot}3$).

3. *The relation between the pressure gradient and the velocity gradient at the wall*

Now we consider the region bounded by the pipe wall and two cross sections apart by a distance $R\,d\theta$. From balance of forces exerted over this portion of the fluid, we have

$$\int_0^{2\pi}\int_0^{a}\left[p - \left(p + \frac{\partial p}{R\,\partial\theta}R\,d\theta\right)\right] r\,dr\,d\psi = -R\,d\theta\,\mu\int_0^{2\pi}\left(\frac{\partial W}{\partial r}\right)_{r=a} a\,d\psi$$

This is written in a non-dimensional form as follows:

$$C = \frac{1}{\pi}\int_0^{2\pi}\left(\frac{\partial w}{\partial \xi}\right)_0 \mathrm{d}\psi = 2\left(\frac{\partial w}{\partial \xi}\right)_{0m} \tag{1.9}$$

As shown later, the variation of δ along ψ is very small, therefore by substituting δ by its mean value δ_m in equation (1.8), the following relation is obtained to compute equation (1.9).

$$\left(\frac{\partial w}{\partial \xi}\right)_0 = \frac{2A}{\delta_m} + \left(\frac{2}{\delta_m} - 1\right)\frac{C}{D}\cos\psi \tag{1.10}$$

From equations (1.9) and (1.10)

$$C = \frac{4A}{\delta_m} \tag{1.11}$$

4. *The boundary-layer momentum equation*

From equation (1.1), the boundary layer equations are derived on the assumption that the thickness of the layer is very thin and both viscous stress and stress by the secondary flow are not ignored. The boundary-layer equation in the direction of the pipe axis is

$$\frac{\partial^2 w}{\partial \xi^2} + u\frac{\partial w}{\partial \xi} - v\frac{\partial w}{\partial \psi} = -C \tag{1.12}$$

Integration of this equation over the boundary layer using the equation of continuity yields the following momentum equations:

$$\left(\frac{\partial w}{\partial \xi}\right)_0 = w_{1\delta}\frac{\partial}{\partial \psi}\int_0^{\delta} v\,\mathrm{d}\xi - \frac{\partial}{\partial \psi}\int_0^{\delta} vw\,\mathrm{d}\xi + \int_0^{\delta} C\,\mathrm{d}\xi + \left(\frac{\partial w}{\partial \xi}\right)_{\delta} \tag{1.13}$$

The right-hand side of equation (1.13) is integrated by using equation (1.8) and reduced as follows after substituting equation (1.11) and replacing δ by δ_m.

$$\left(\frac{\partial w}{\partial \xi}\right)_0 = E + F\cos\psi \tag{1.14}$$

where

$$E = \left\{\left(\frac{2}{5} - \frac{13}{15}\delta_m\right)\cos^2\psi + \left(\frac{3}{5} - \frac{17}{15}\delta_m\right)\sin^2\psi + \delta_m\right\}C \tag{1.15}$$

$$F = \left\{\frac{D\delta_m}{4}\left(\frac{2}{5} - \frac{4}{15}\delta_m\right) - \frac{1}{D}\right\}C \tag{1.16}$$

The mean value of equation (1.14) over ψ is $C/2$ and satisfies equation (1.9). Equation (1.14) must be equal to equation (1.10). Equation (1.10) has a simple form as it was reduced from a plain velocity profile in the core region given by equation (1.6), while E in equation (1.14) is a function of ψ.

However, the variation of E with ψ is very small compared with that of the rest terms in equation (1.14) as shown in Fig. 5, therefore E is taken to be constant and replaced with its mean value $C/2$. Then in order to let equation (1.10) be equal to equation (1.14) the coefficient of $\cos\psi$ in equation (1.10) must be equated with F, and the following relation between D and δ_m is found:

$$\left(\frac{1}{5} - \frac{2}{15}\delta_m\right)D^2\delta_m^2 = 4 \tag{1.17}$$

In Adler's and others' reports, they did not take into account this analysis in the momentum balance and introduced discontinuity of tangential velocity at the edge of the boundary layer, therefore they unreasonably had finite tangential velocity in the boundary layer at $\psi = \pi$.

In order to determine D and δ_m, another relation between them is introduced by considering momentum balance in the radial and circumferential direction in the boundary layer. The momentum equations are

$$\left.\begin{aligned} P &= \int_{\xi}^{\delta}\left(v^2 + \frac{w^2}{H}\cos\psi\right)\mathrm{d}\xi + P_{\delta} \\ &\frac{\partial}{\partial \psi}\int_0^{\delta} v^2\,\mathrm{d}\xi - v_1\frac{\partial}{\partial \psi}\int_0^{\delta} v\,\mathrm{d}\xi + \\ &\frac{\sin\psi}{H}\int_0^{\delta} w^2\,\mathrm{d}\xi + \int_0^{\delta}\frac{\partial P}{\partial \psi}\mathrm{d}\xi + \\ &\left(\frac{\partial v}{\partial \xi}\right)_0 = 0 \end{aligned}\right\} \tag{1.18}$$

In the equation obtained by substituting equation (1.8) into these equations, A and C are included. To express A and C by δ_m, the flow

rate through the pipe is considered in terms of the average velocity defined as follows:

$$w_m = \frac{Re}{2} = \frac{1}{\pi}\left\{\int_0^{2\pi}\int_0^{1-\delta} w_1\eta \, d\eta \, d\psi + \int_0^{2\pi}\int_0^{\delta} w(1-\xi) \, d\xi \, d\psi\right\} \tag{1.19}$$

where

$$Re = 2a \, W_m/\nu.$$

When we substitute equations (1.6) and (1.8) into equation (1.19), integrate it and replace δ by δ_m, we get

$$A = \frac{Re}{2} \frac{1}{1 - \frac{2}{3}\delta_m + \frac{1}{6}\delta_m^2} \tag{1.20}$$

From equation (1.11), we have

$$C = \frac{2Re}{\delta_m} \frac{1}{1 - \frac{2}{3}\delta_m + \frac{1}{6}\delta_m^2} \tag{1.21}$$

Substituting equations (1.6) and (1.8) into (1.18) and using equations (1.20) and (1.21), we have

$$\left.\begin{aligned} &\frac{1}{35}(96 - 77\delta - 23\delta^2 + \\ &43\delta^3)D^4\delta_m^2\delta\cos\psi\left(1 - \frac{2}{3}\delta_m + \right. \\ &\left.\frac{1}{6}\delta_m^2\right)^2 + \frac{K^2}{4}\delta^3\left[\left(-\frac{14}{30} + \right.\right. \\ &\left.\delta\right)\left\{D\delta_m + 4(1-\delta)\cos\psi\right\}^2 + \\ &\frac{28}{30}\delta\left\{D\delta_m + 4(1-\delta)\cos\psi\right\}\cos\psi + \\ &\left.\frac{16}{30}\delta^2\cos^2\psi\right] - \frac{11K^2}{30}\delta^4\left(\frac{1}{4}D^2\delta_m^2 + \right. \\ &\left.4D\delta_m\cos\psi + 12\cos^2\psi\right) + \\ &D^3\delta_m^2(12 - 6\delta)\left(1 - \frac{2}{3}\delta_m + \right. \\ &\left.\frac{1}{6}\delta_m^2\right)^2 = 0 \end{aligned}\right\} \tag{1.22}$$

where

$$K = Re/\sqrt{H}[\equiv Re\sqrt{(a/R)}]$$

5. *Computation of D and* δ_m

In this report phenomena in the region of large Dean number K are analysed. According to the high approximation in the boundary-layer theory D and δ may be expanded in a power series of $K^{-1/2}$. Moreover δ is expressed by its mean value δ_m and the deviation $\Delta\delta$. It can be easily shown from the investigation of the power of K in equation (1.17) and equation (1.22) that the series of D start with $K^{1/2}$ and δ with $K^{-1/2}$. Thus D and δ are expanded as

$$\left.\begin{aligned} D &= D_1 K^{1/2} + D_2 + D_3 K^{-1/2} + \dots \\ \delta &= (\delta_{m1} + \Delta\delta_1) K^{-1/2} + (\delta_{m2} + \\ &\qquad \Delta\delta_2) K^{-1} + \dots \end{aligned}\right\} \tag{1.23}$$

Then substitution of equation (1.23) in equations (1.17) and (1.22) and equating of coefficients of the same power of K give D and δ_m as follows:

(*a*) *1st approximation.* Equating the coefficients of K^0 in equation (1.17), we find

$$D_1^2 \delta_{m1}^2 = 20 \tag{1.24}$$

If we equate the coefficients of $K^{1/2}$ in equation (1.22), we have

$$\frac{96}{35}D_1^2(\delta_{m1} + \Delta\delta_1)\cos\psi + 12 D_1 - \frac{7}{60}(\delta_{m1} + \Delta\delta_1)^3\left(1 + \frac{4}{D_1\delta_{m1}}\cos\psi\right)^2 = 0 \tag{1.25}$$

This equation contains the constant terms and the terms varying with ψ. Considering only the constant terms in equation (1.25), we have

$$\delta_{m1}^3 = \frac{720}{7} D_1 \tag{1.26}$$

From equations (1.24) and (1.26), D_1 and δ_{m1} are determined as follows

$$\left.\begin{aligned} D_1 &= 0{\cdot}965\,6 \\ \delta_{m1} &= 4{\cdot}631\,1 \end{aligned}\right\} \tag{1.27}$$

Use of these values gives the distribution of δ along ψ from equation (1.25) as shown in Fig. 4. The figure shows that the variation of δ

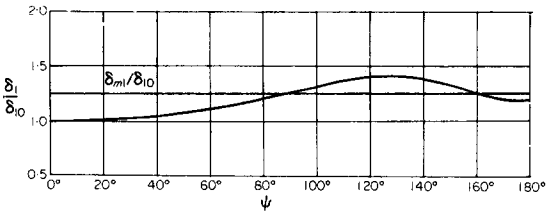

FIG. 4. Distribution of δ along ψ. (δ_{10} is δ_1 at $\psi = 0°$.)

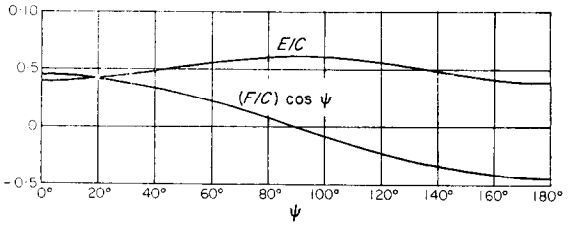

FIG. 5. Comparison of E and $F\cos\psi$ in equations (1-14).

with ψ is considerably small. From the values of D_1 and δ_{m1}, E and $F\cos\psi$ of equation (1.15) and equation (1.16) are computed and shown in Fig. 5. The figure shows that the variation of E with ψ is small compared with $F\cos\psi$ as assumed in the previous analysis.

(*b*) *2nd approximation.* Equation (1.28) is derived by equating the coefficients of $K^{1/2}$ in equation (1.17) and using equation (1.27).

$$8{\cdot}284\ D_2 + 1{\cdot}727\ \delta_{m2} = 12{\cdot}35 \qquad (1.28)$$

We get also the following equation by equating the coefficients of K^0 in equation (1.22):

$$240{\cdot}0\ D_2 - 150{\cdot}1\ \delta_{m2} = 511{\cdot}1 \qquad (1.29)$$

From these two equations D_2 and δ_{m2} are determined as follows:

$$\left.\begin{aligned} D_2 &= 1{\cdot}650 \\ \delta_{m2} &= -\ 0{\cdot}765\ 9 \end{aligned}\right\} \qquad (1.30)$$

(6) *The resistance coefficient*

The definition of a resistance coefficient for a curved pipe is

$$\lambda_c = \left(-\frac{\partial p}{R\partial\theta}\right)\cdot\frac{2a}{\frac{1}{2}\rho W_m^2}$$

This is written as

$$\lambda_c = C\cdot\frac{16}{Re^2} \qquad (1.31)$$

With the resistance coefficient for a straight pipe $\lambda_s = (64/Re)$, the resistance coefficient ratio is given by

$$\frac{\lambda_c}{\lambda_s} = \frac{C}{4Re} = \frac{A}{\delta_m\, Re} \qquad (1.32)$$

The first approximation of this ratio is obtained by putting $\delta_m = \delta_{m1}\, K^{-1/2}$ and $A = Re/2$ as follows:

$$\left(\frac{\lambda_c}{\lambda_s}\right)_{\mathrm{I}} = \frac{K^{1/2}}{2\,\delta_{m1}} = 0{\cdot}108\ 0\ K^{1/2} \qquad (1.33)$$

Use of δ_{m2} and

$$A = \frac{Re}{2\,(1 - \frac{2}{3}\,\delta_m)}$$

gives the correction factor for the second approximation as

$$\left(\frac{\lambda_c}{\lambda_s}\right)_{\mathrm{II}} = \left(\frac{\lambda_c}{\lambda_s}\right)_{\mathrm{I}}\cdot\frac{1}{1 - 3{\cdot}253\ K^{-1/2}} \qquad (1.34)$$

where the suffixes I and II indicate respectively values by the first and second approximation.

As shown in Fig. 6, in a wide range of Dean

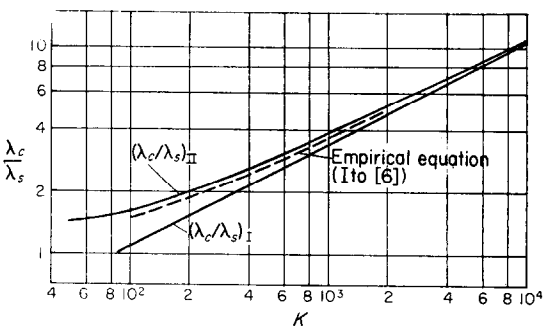

FIG. 6. $\frac{\lambda_c}{\lambda_s} - K$ diagram.

number K equation (1.34) agrees fairly well with the following empirical formulae provided by Ito [6]:

$$\frac{\lambda_c}{\lambda_s} = \frac{21{\cdot}5\,K}{[1{\cdot}56 + \log K]^{5{\cdot}73}} \qquad (1.35)$$

$$2000 > K > 13{\cdot}5$$

Theoretical investigation by Dean [7] is limited in a Dean number region smaller than 36 and the difference of resistance coefficient from that in a straight pipe is practically negligible. The flow pattern by his analysis is shown in Fig. 8 and differs from that in a large Dean number region which is obtained in this report as shown in Fig. 7.

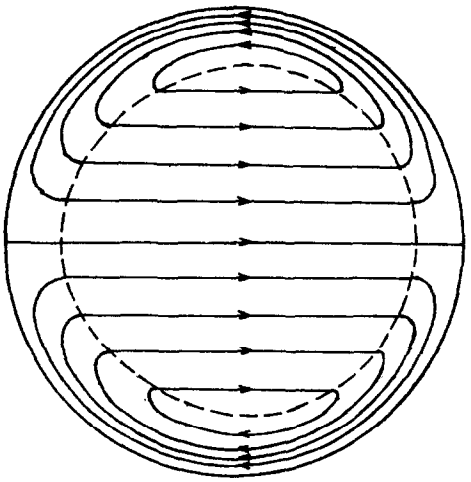

FIG. 7. Flow pattern of the secondary flow in the case of large K.

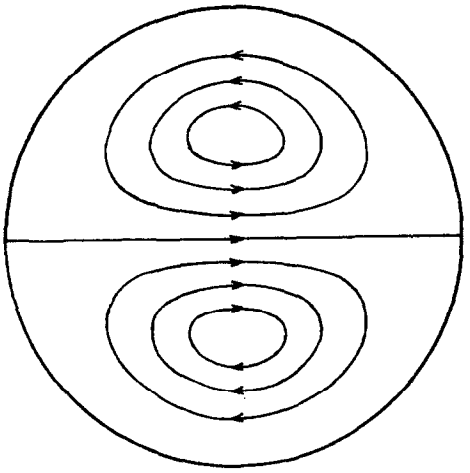

FIG. 8. Flow pattern of the secondary flow in the case of small K.

LAMINAR HEAT TRANSFER IN A CURVED PIPE

For fully developed flow under the condition of uniform heat flux, the temperature T can be expressed in the form

$$T = \tau R\theta - G(r, \psi)$$

where τ is a constant temperature gradient along the pipe axis.

Seban and McLaughlin [5] observed the temperature distribution around the periphery of cross section of the pipe. However, for laminar flow, this difference is very small and may be considered to be negligible even in the case of a pipe having such a thin wall as in their experiments for the purpose of obtaining the mean Nusselt number around the periphery. According to our experiments shown below which were carried out with air flowing through the pipe having a relatively thick wall, the peripheral temperature distribution was observed to be almost negligible.

Therefore in the following analysis the temperature of a pipe wall is assumed to be constant around the periphery, then the wall temperature is indicated by

$$T_w = \tau R\theta.$$

When r/R is so small as assumed in the flow field analysis the energy equation in a non-dimensional form becomes

$$\frac{\partial}{\eta\,\partial\eta}(\eta q_\eta) + \frac{\partial q_\psi}{\eta\,\partial\psi} = w \tag{2.1}$$

where

$$\left.\begin{aligned} q_\eta &= -\frac{1}{Pr}\frac{\partial g}{\partial\eta} + ug \\ q_\psi &= -\frac{1}{Pr\,\eta}\frac{\partial g}{\partial\psi} + vg \end{aligned}\right\} \tag{2.2}$$

The first terms in the right-hand side of equation (2.2) express conduction heat and the second terms mean convection heat. The secondary flow introduces additional convection heat. In a large Dean number region the secondary motion is strong enough, and then it is considered that the contribution of the secondary flow to heat transfer is predominant in the core region of the cross section except for a thin layer near to the

pipe wall. The secondary flow tends to make the temperature distribution uniform in the core region, while in the region adjacent to the wall steep temperature gradient might exist.

1. *The temperature field in the core region*

If we replace g by g_1 in the core region, we get from equation (2.2)

$$q_\eta = u_1 g_1, \quad q_\psi = v_1 g_1 \tag{2.3}$$

From equation (2.1), the following energy equation is obtained;

$$u_1 \frac{\partial g_1}{\partial \eta} + v_1 \frac{\partial g_1}{\eta \partial \psi} = w_1 \tag{2.4}$$

Substitution of equation (1.6) for u_1, v_1, w_1 in this equation yields g_1 as

$$g_1 = A' + \frac{C}{2D^2}\eta^2 + \frac{A}{D}\eta \cos\psi \tag{2.5}$$

2. *The temperature distribution in the region adjacent to the wall*

We assume along the wall a thermal boundary layer of thickness δ_t. The thickness δ_t is regarded as one of main parameters determining the temperature gradient at the wall. When the thermal boundary layer is assumed to be less thick than the boundary layer of the flow, the temperature profile in the boundary layer must be taken so as to meet the temperature at the edge of the core region, that is $\xi = \delta$, and let the temperature gradient at the wall be dependent on δ_t. Hence when $\delta_t < \delta$, the temperature profile in the thermal boundary layer is written in the following form satisfying the boundary conditions

$$g = g_{1\delta}, \quad \frac{\partial g}{\partial \xi} = -\left(\frac{\partial g_1}{\partial \eta}\right)_\delta \quad \text{at } \xi = \delta$$

$$\left.\begin{aligned} g = g_{1\delta}\Bigg\{ & \frac{2}{\zeta}\left(\frac{\xi}{\delta} - 2\frac{\xi^2}{\delta^2} + \frac{\xi^3}{\delta^3}\right) + 3\frac{\xi^2}{\delta^2} - \\ & 2\frac{\xi^3}{\delta^3}\Bigg\} + \delta\Bigg\{\frac{C}{D^2}(1-\delta) + \\ & \frac{A}{D}\cos\psi\Bigg\}\left(\frac{\xi^2}{\delta^2} - \frac{\xi^3}{\delta^3}\right) \end{aligned}\right\} \tag{2.6}$$

where

$$\zeta = \delta_t/\delta.$$

On the contrary, when $\delta_t > \delta$, the temperature profile is taken to meet the temperature of the core region at the edge of the thermal boundary layer. In this case the boundary conditions are

$$g = g_{1\delta_t}, \quad \frac{\partial g}{\partial \xi} = -\left(\frac{\partial g_1}{\partial \eta}\right)_{\delta_t} \quad \text{at } \xi = \delta_t.$$

Therefore we take the following temperature profile:

$$g = g_{1\delta_t}\left(2\frac{\xi}{\delta_t} - \frac{\xi^2}{\delta_t^2}\right) + \delta_t\left\{\frac{C}{D^2}(1-\delta_t) + \frac{A}{D}\cos\psi\right\}\left(\frac{\xi^2}{\delta_t^2} - \frac{\xi^3}{\delta_t^3}\right) \tag{2.7}$$

3. *Relation among the mean temperature gradient at the wall, Reynolds number and Prandtl number*

Heat balance over the region bounded by the pipe wall and two cross sections apart by a distance $R\,d\theta$ is expressed by the following equation.

$$k\int_0^{2\pi}\left(\frac{\partial T}{\partial r}\right)_{r=a} a\,d\psi = \rho c_p \int_0^{2\pi}\int_0^a \frac{\partial}{R\,\partial\theta}(wT)\,r\,dr\,d\psi$$

In dimensionless form, this becomes

$$\frac{1}{Pr}\int_0^{2\pi}\left(\frac{\partial g}{\partial \xi}\right)_0 d\psi = \int_0^{2\pi}\int_0^1 w\eta\,d\eta\,d\psi = \frac{\pi}{2}Re \tag{2.8}$$

The following relation is obtained by using the mean value:

$$\left(\frac{\partial g}{\partial \xi}\right)_{0m} = \frac{Re\,Pr}{4} \tag{2.9}$$

To calculate equation (2.9) from equations (2.6) and (2.7) δ and δ_t are replaced by δ_m and δ_{tm} respectively based on their little dependence of ψ. If δ_m and δ_{tm} are assumed to be negligibly small compared with unity, we have the following relation for $\delta_t \lesssim \delta$:

$$\left(\frac{\partial g}{\partial \xi}\right)_0 = \frac{2}{\zeta\delta_m}\left(A' + \frac{Re}{D^2\,\delta_m}\right) + \frac{Re}{\zeta\,D\,\delta_m}\cos\psi \tag{2.10}$$

Then the following relation is obtained from this equation:

$$A' = \frac{\zeta\,\delta_m\,Re\,Pr}{8} - \frac{Re}{D^2\,\delta_m} \tag{2.11}$$

4. *The energy integral equation of the boundary layer*

In the boundary layer, the conduction terms and the convection terms due to secondary flow are considered to be of the same order of magnitude. By the boundary layer approximation the energy equation is written as

$$-\frac{1}{Pr}\frac{\partial^2 g}{\partial \xi^2} - u\frac{\partial g}{\partial \xi} + v\frac{\partial g}{\partial \psi} - w = 0 \tag{2.12}$$

(*a*) *For the case of* $\delta_t < \delta$. In this case the integration has to be done from $\xi = 0$ to $\xi = \delta$. The energy integral equation is reduced to

$$\frac{1}{Pr}\left(\frac{\partial g}{\partial \xi}\right)_0 = g_{1\delta}\frac{\partial}{\partial \psi}\int_0^{\delta} v\,d\xi - \frac{\partial}{\partial \psi}\int_0^{\delta} gv\,d\xi + \int_0^{\delta} w\,d\xi \tag{2.13}$$

By substituting equations (1.8) and (2.6) into this equation, putting $A = Re/2$ and neglecting smaller terms the temperature gradient at the wall is obtained as follows.

$$\left.\begin{aligned}&\left(\frac{\partial g}{\partial \xi}\right)_0 = \frac{Re\,Pr}{2}\left\{\left(\frac{22}{35} - \frac{8}{35\zeta}\right)\cos^2\psi + \left(\frac{8}{35\zeta} + \frac{13}{35}\right)\sin^2\psi\right\} + \\ &\frac{\zeta\,D\,\delta_m\,Re\,Pr^2}{8}\left(\frac{22}{35} - \frac{8}{35\zeta}\right)\cos\psi \\ &= M + N\cos\psi\end{aligned}\right\} \tag{2.14}$$

The mean value of this equation over ψ satisfies the relation (2.9). Equation (2.10) consists of the constant term and the term varying with $\cos\psi$, where the constant term is equal to $Re\,Pr/4$. The variation of M with ψ is very small and M in equation (2.14) is replaced by its mean value. From comparison of N with coefficient of $\cos\psi$ in equation (2.10), we have

$$\frac{\zeta\,D\,\delta_m\,Re\,Pr^2}{8}\left(\frac{22}{35} - \frac{8}{35\zeta}\right) = \frac{Re}{\zeta\,D\,\delta_m}$$

Thus the following relation between the thickness ratio and the Prandtl number is obtained by putting $D^2\delta_m^2 \approx 20$ from equation (1.24).

$$\zeta = \frac{2}{11}\left[1 + \sqrt{\left(1 + \frac{77}{4}\cdot\frac{1}{Pr^2}\right)}\right] \tag{2.15}$$

In equation (2.15) $\zeta \leqslant 1$ corresponds to $Pr \geqslant 1$.

This equation indicates that for very large Prandtl number ζ approaches to an asymptotic value of 4/11 and δ_t tends to its limit.

(*b*) *For the case of* $\delta_t > \delta$. In this case, when equation (2.12) is integrated from $\xi = 0$ to $\xi = \delta_t$ the energy integral equation becomes

$$\frac{1}{Pr}\left(\frac{\partial g}{\partial \xi}\right)_0 = g_{1\delta_t}\frac{\partial}{\partial \psi}\int_0^{\delta_t} v\,d\xi - \frac{\partial}{\partial \psi}\int_0^{\delta_t} gv\,d\xi + \int_0^{\delta_t} w\,d\xi \tag{2.16}$$

The same procedure as shown in the case of $\delta_t < \delta$ is applicable to this case. When the first order terms are taken into account, the following expression of the temperature gradient at the wall is obtained:

$$\left.\begin{aligned}&\left(\frac{\partial g}{\partial \xi}\right)_0 = \frac{Re\,Pr}{2}\left\{\left(1 - \frac{4}{5\zeta} + \frac{1}{5\zeta^2}\right)\cos^2\psi + \left(\frac{4}{5\zeta} - \frac{1}{5\zeta^2}\right)\sin^2\psi\right\} + \\ &\frac{\zeta\,D\,\delta_m\,Re\,Pr^2}{8}\left(1 - \frac{4}{5\zeta} + \frac{1}{5\zeta^2}\right)\cos\psi\end{aligned}\right\} \tag{2.17}$$

If the terms in the first bracket are replaced by the mean value $\frac{1}{2}$, this equation comes to be same in the form with equation (2.10). By equating the coefficients of $\cos\psi$, we have

$$\zeta = \frac{1}{5}\left[2 + \sqrt{\left(\frac{10}{Pr^2} - 1\right)}\right] \tag{2.18}$$

In this case $\zeta \geqslant 1$, corresponds to $Pr \leqslant 1$.

5. *Nusselt numbers*

The definition of Nusselt number is given by

$$Nu = \frac{2a\,.\,q}{k\,(T_w - T_m)}$$

The Nusselt number for a straight pipe is 48/11, therefore the ratio of Nusselt number for a curved pipe to that for a straight pipe is written that

$$\frac{Nu_c}{Nu_s} = \frac{11}{48} \cdot \frac{2a \cdot q}{k\,(T_w - T_m)} \tag{2.19}$$

Where q is a heat input from the pipe wall per unit area and unit time. From equation (2.8), the heat input per unit length of the pipe and unit time is found that

$$-k \int_0^{2\pi} \left(\frac{\partial T}{\partial r}\right)_{r=a} a\,\mathrm{d}\psi = 2\pi ak\tau \left(\frac{\partial g}{\partial \xi}\right)_{0m} = \frac{\pi}{2}\tau ak\,Re\,Pr$$

Therefore q is given by

$$q = \tfrac{1}{4}\tau k Re\,Pr \tag{2.20}$$

The mixed mean temperature T_m is defined as

$$T_m = \frac{1}{\pi a^2 W_m} \int_0^{2\pi} \int_0^{a} T \cdot W \cdot r\,\mathrm{d}r\,\mathrm{d}\psi$$

when $\delta_t > \delta$

$$T_w - T_m = \frac{2}{\pi}\frac{\tau a}{Re}\left\{ \int_0^{2\pi} \int_0^{1-\delta_t} g_1 w_1 \eta\,\mathrm{d}\eta\,\mathrm{d}\psi + \int_0^{2\pi} \int_{\delta}^{\delta_t} g\,w_1 (1-\xi)\,\mathrm{d}\xi\,\mathrm{d}\psi + \int_0^{2\pi} \int_0^{\delta} g\,w\,(1-\xi)\,\mathrm{d}\xi\,\mathrm{d}\psi \right\} \tag{2.22}$$

Substitution of equations (2.20), (2.21) or (2.22) into equation (2.19) yields the Nusselt number ratio expressed as a function of Dean number K and thickness ratio ζ.

In the first approximation, the Nusselt number ratio is given for both cases by

$$\left(\frac{Nu_c}{Nu_s}\right)_{\mathrm{I}} = 0{\cdot}197\,9\,\frac{K^{1/2}}{\zeta} \tag{2.23}$$

The second approximation is obtained by correcting the first approximation with the temperature and the velocity distributions in the boundary layer and taking into account of terms of the order of magnitude K^{-1}.

For the case $\delta_t \leqslant \delta$, i.e. $Pr \geqslant 1$

$$\left(\frac{Nu_c}{Nu_s}\right)_{\mathrm{II}} = \left(\frac{Nu_c}{Nu_s}\right)_{\mathrm{I}} \cdot \frac{1}{1 + \dfrac{37{\cdot}05}{\zeta}\left\{\dfrac{1}{40} - \dfrac{17}{120}\zeta + \left(\dfrac{1}{10\zeta} + \dfrac{13}{30}\right)\dfrac{1}{10\,Pr}\right\} K^{-1/2}} \tag{2.24}$$

For the case $\delta_t \geqslant \delta$, i.e. $Pr \leqslant 1$

$$\left(\frac{Nu_c}{Nu_s}\right)_{\mathrm{II}} = \left(\frac{Nu_c}{Nu_s}\right)_{\mathrm{I}} \cdot \frac{1}{1 - \dfrac{37{\cdot}05}{\zeta}\left\{\dfrac{\zeta^2}{12} + \dfrac{1}{24} - \dfrac{1}{120\zeta} - \left(\dfrac{4}{3}\zeta - \dfrac{1}{3\zeta} + \dfrac{1}{15\zeta^2}\right)\dfrac{1}{20\,Pr}\right\} K^{-1/2}} \tag{2.25}$$

Use of the dimensionless quantities gives the difference between the wall temperature and the mixed mean temperature as

when $\delta_t < \delta$

$$T_w - T_m = \frac{2}{\pi}\frac{\tau a}{Re}\left\{ \int_0^{2\pi} \int_0^{1-\delta} g_1 w_1 \eta\,\mathrm{d}\eta\,\mathrm{d}\psi + \int_0^{2\pi} \int_0^{\delta} g\,w(1-\xi)\,\mathrm{d}\xi\,\mathrm{d}\psi \right\} \tag{2.21}$$

The thickness ratio ζ is given by equation (2.15) for the case $Pr \geqslant 1$, and equation (2.18) for the case $Pr \leqslant 1$. Some examples of the relation of the Nusselt number ratio against Dean number K are shown in Fig. 9. For $Pr = 0{\cdot}71$ and ∞, the curve of $(Nu_c/Nu_s)_{\mathrm{II}}$ is also shown. From the curves of $(Nu_c/Nu_s)_{\mathrm{I}}$ and $(Nu_c/Nu_s)_{\mathrm{II}}$, it is possible to predict the effect of curvature on Nusselt number for any Prandtl number. For large Prandtl numbers the Nusselt number ratio tends to depend only on the

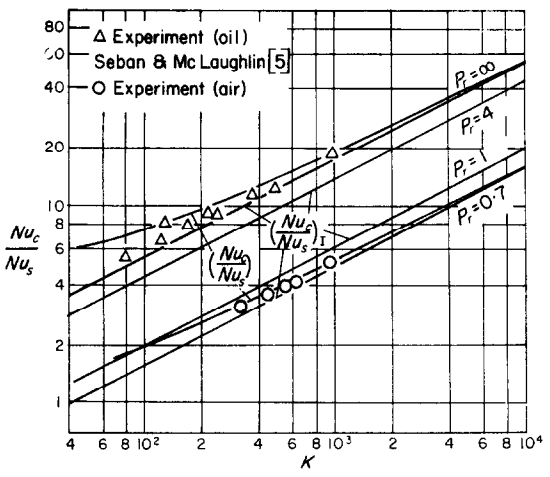

FIG. 9. $\frac{Nu_c}{Nu_s} - K$ diagram.

intensity of the secondary flow and come to show little change with Prandtl number. The experimental data for air obtained by our experiments are in good agreements with the curve for $Pr = 0{\cdot}71$. Some examples of the data for oil reported by Seban and McLaughlin [5] are also plotted taking mean value of Nusselt numbers at the inner and the outer wall. For lack of exact information about the Prandtl number at each run, the data are plotted assuming $Pr = 400$.

EXPERIMENTS

The schematic diagram of the experimental apparatus is shown in Fig. 10. A curved pipe of the radius ratio of 40 was used. The pipe is of brass, and 35·6 mm in an inside diameter and 1·2 mm in a wall thickness. Upstream of the curved pipe placed in a horizontal plane a straight pipe of 8·55 m long is provided to settle the flow fully. The air supplied by a blower flows through a metering orifice for flow rate measurement, a settling chamber, the straight section and the curved pipe, and is discharged to open air.

The flow rate is measured by means of a orifice and a Betz type manometer. The pipe is electrically heated by nichrom wire wound around it. The heating wire is divided into four parts which are separately controlled by four transformers so as to maintain the constant temperature gradient along the pipe axis. The wire is electrically insulated from the pipe by a thin rock wool tape covering the pipe wall. The wall temperature is measured at six stations as

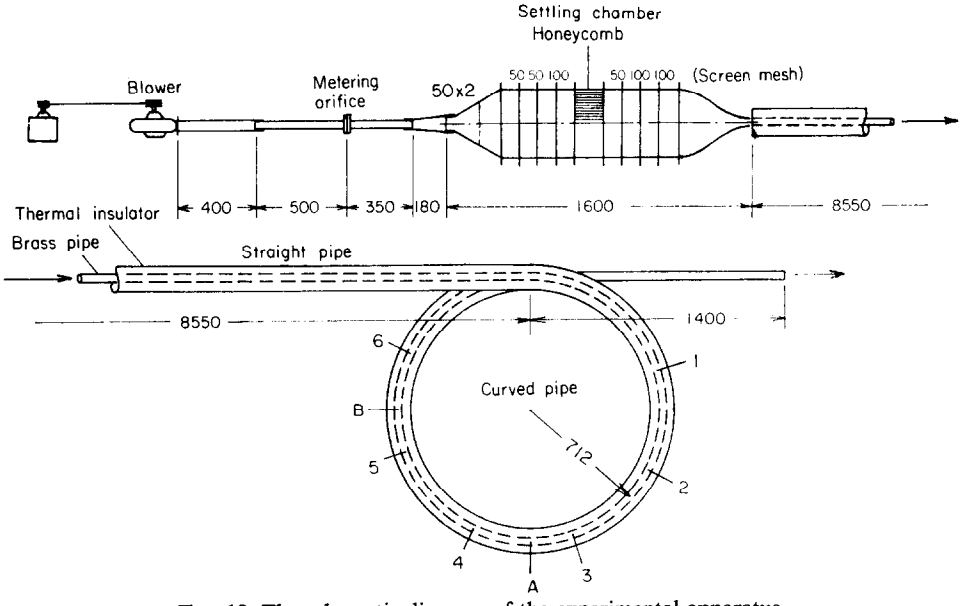

FIG. 10. The schematic diagram of the experimental apparatus.

shown in Fig. 10 by thermocouples attached to the external surface of the pipe. At the station 2 and 5, in order to see the temperature variation around the periphery four thermocouples are attached at the top, bottom and each side. The velocity and temperature distributions inside the pipe are measured at two stations, A and B in Fig. 10, by traversing probes horizontally or vertically through holes or slits at the pipe wall. The velocity distributions are measured by means of an one-hole cylindrical yaw probe and a Chattock type manometer. The probe is of stainless steel, and is 0·8 mm in a diameter. It has a pressure hole of 0·2 mm diameter. The probe is inserted thoroughly from one side of the wall to the other side. To measure the velocity at a position, the stagnation pressure is measured at first, and then according to the calibrated characteristics the static pressure is measured by rotating the probe around its axis to the angle of 43 degrees from the flow direction.

The temperature distributions are measured by means of a T-shaped thermocouple probe and a potentiometer. The traversing device and a detailed figure of the probe are shown in Fig. 11.

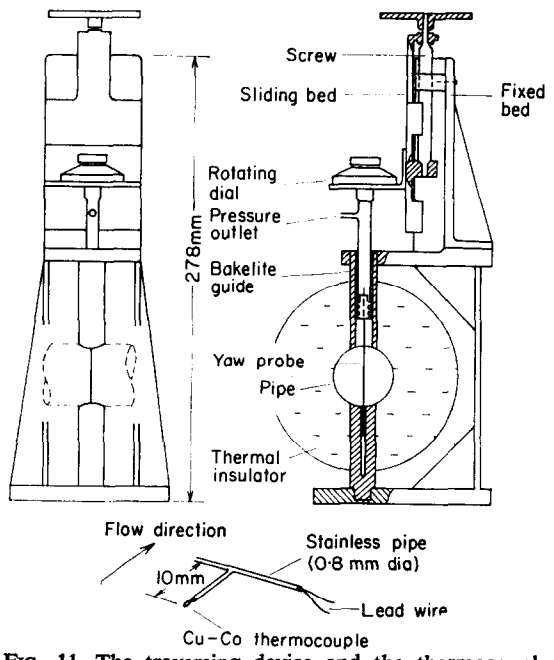

FIG. 11. The traversing device and the thermocouple probe.

The velocity distributions in a horizontal plane at two different sections where the flow fully developed and was ascertained to be laminar by a hot wire anemometer are shown in Fig. 12. As Ito reported, our experiment also reveals

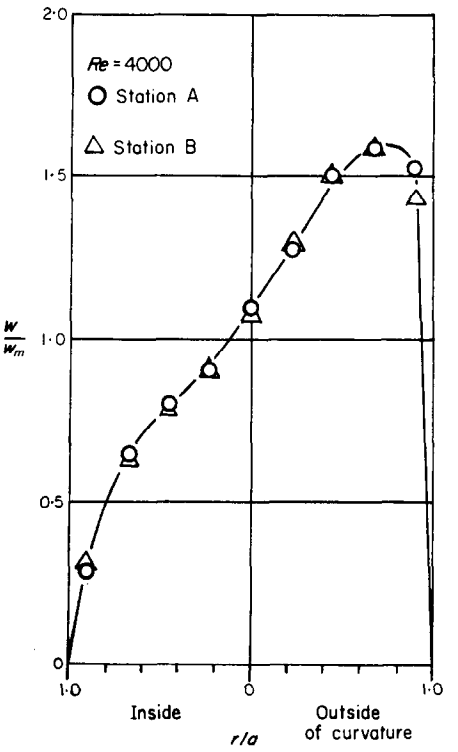

FIG. 12. Comparison of the velocity profiles measured at station *A* and *B* in Fig. 10.

that the flow develops in a short running length in a curved pipe and detailed measurements were carried out for fully developed flows. Figure 13 shows that velocity profiles are not influenced by heating as assumed in the theoretical analysis. In Fig. 14 velocity profiles in horizontal and vertical planes are shown with the Poiseuille profile. Observed temperature profiles in a horizontal plane are shown in Fig. 15 to reveal that they are fully developed. In Fig. 16 similar to velocity profile, temperature profiles in a vertical and horizontal plane are plotted with that calculated by using the Poiseuille velocity profile.

These observed velocity and temperature profiles make clear that, as assumed in the

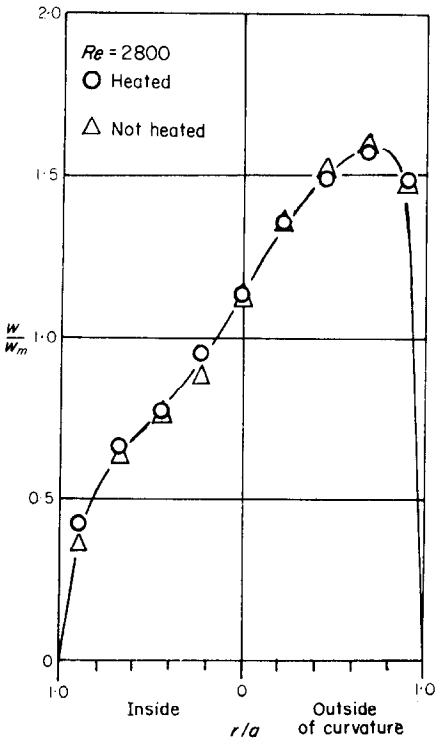

FIG. 13. Comparison of the velocity profiles measured when the pipe was heated and not heated.

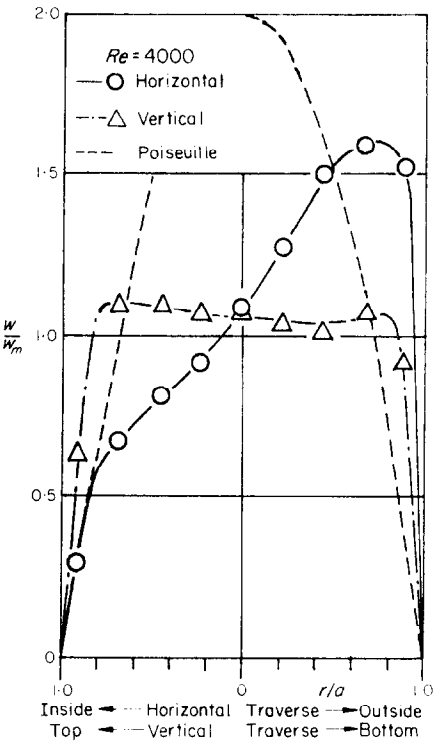

FIG. 14. Velocity profiles.

theoretical analysis, only in the region close to the wall velocity and temperature gradient are so large as observed in a boundary layer around a body.

Heat input is evaluated from equation (2.20) where a temperature gradient is obtained from measurement of wall temperatures. A mixed mean temperature is evaluated as follows. A cross section of the pipe is divided into small meshes as shown in Fig. 17. By use of the velocity W_{i0}, W_{0j} and the temperature T_{i0}, T_{0j} measured on horizontal and vertical planes passing through a center of the section, the velocity and the temperature in a mesh (x_i, y_j) are calculated by

$$W_{ij} = \frac{W_{i0}\, W_{0j}}{W_0}$$

$$T_{ij} = \frac{T_{i0} \cdot T_{0j}}{T_0}$$

where W_0 and T_0 are the velocity and the temperature at the center of the section. Then the mixed mean temperature is calculated by

$$T_m = \frac{\sum_{ij} W_{ij}\, T_{ij}\, \mathrm{d}x_i\, \mathrm{d}y_j}{\sum_{ij} W_{ij}\, \mathrm{d}x_i\, \mathrm{d}y_j}$$

The Nusselt number ratio is obtained from equation (2.19) and heat input determined from the measured wall temperature gradient. The physical property is evaluated at the mixed mean temperature. The results are in good agreements with the theoretical evaluation as shown in Fig. 9.

CONCLUSION

In the range of very large Dean number $K = Re\sqrt{a/R}$, a flow field and a temperature field in a curved pipe are analysed for fully developed laminar flow with constant heat flux by theory and experiment, and the following conclusive results are obtained.

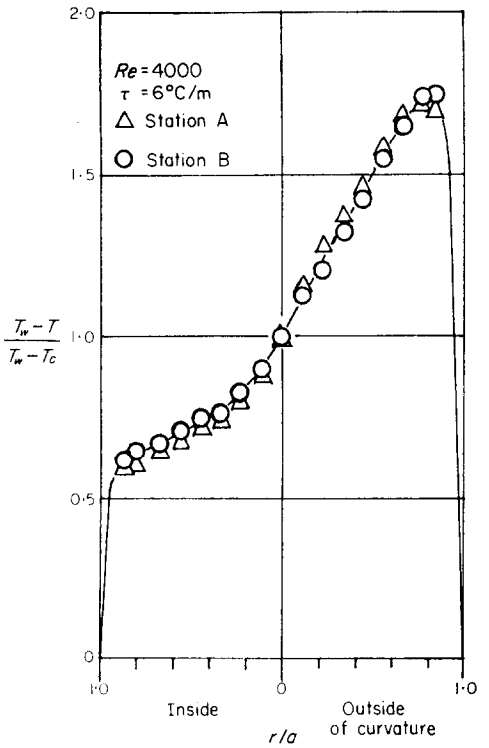

FIG. 15. Comparison of the temperature profiles measured at station A and B in Fig. 10. (T_c is the temperature at the centre of the pipe.)

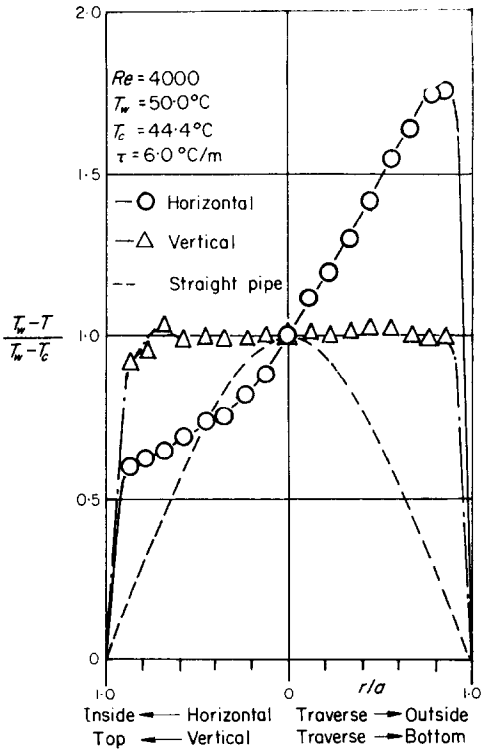

FIG. 16. Temperature profiles. (T_c is the temperature at the centre of the pipe.)

(1) The flow field is divided into the core region and the boundary layer along the wall. The additive flow resistance in a curved pipe was shown to be caused by stresses due to the secondary flow. The result which was obtained by theoretical analysis to the second approximation was found to agree with the experimental results obtained so far.

(2) The same procecure as for the flow field is applied to the analysis of heat transfer in a fully developed temperature field under the condition of uniform heat flux. The ratio of thickness of a temperature boundary layer to that of a velocity boundary layer was expressed in the terms of Pr number. Nu number was shown to be a function of Dean number with a parameter of Pr number.

(3) Experiment was carried out for a fully developed laminar air flow in a curved pipe of $R/a = 40$ and of 35·6 mm inner diameter in the measurement of velocity and temperature profile.

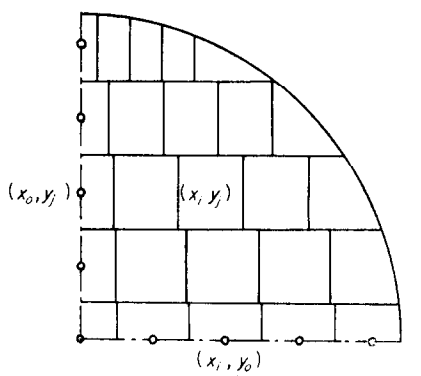

FIG. 17. The cross section of the pipe divided into small meshes in order to calculate a mixed mean temperature.

The experimental results about these profiles supported the boundary-layer approximation applied in the theoretical analysis.

Nusselt numbers calculated from experimental data were shown to agree with those obtained theoretically.

REFERENCES

1. D. JESCHKE, Wärmeübergang und Druckverlust in Rohrschlagen, *Z. Ver. Deut. Ing.* **69**, 1526 (1925); *Z. V.D.I.* **24**, 1 (1925).
2. F. MERKEL, *Die Grundlagen der Wärmeübertragung*, p. 51. Steinkopf, Leipzig (1927).
3. W. B. HAWES, Some sidelights on the heat transfer problem, *Trans. Instn Chem. Engrs, Lond.* **10**, 161–167 (1932).
4. A. J. EDE, The effect of a right-angled bend on heat transfer in a pipe. *International Developments in Heat Transfer*, 634–642 (1961).
5. R. A. SEBAN and E. F. MCLAUGHLIN, Heat transfer in tube coils with laminar and turbulent flow, *Int. J. Heat Mass Transfer* **6**, 387–395 (1963).
6. H. ITO, Friction factors for turbulent flow in curved pipes, *J. Basic Engng, Trans. Amer. Soc. Mech. Engrs* **D81**, 123–134 (1959); For laminar flow, see—Theoretical and experimental investigation concerning the flow through curved pipes, *Mem. Inst. High Speed Mechanics, Tohoku Univ., Japan* **14**, 137–172 (1959).
7. W. R. DEAN, Note on the motion of fluid in a curved pipe, *Phil. Mag.* **4**, 208–223 (1927); *Phil. Mag.* **5**, 673–695 (1928).
8. M. ADLER, Strömung in gekrümmten rohren, *Z. Angew. Math. Mech.* **14**, 257–275 (1934).
9. S. N. BARUA, On secondary flow in stationary curved pipes, *Quart. J. Mech. Appl. Math.* **16**, 61–77 (1962).

Résumé—L'étude théorique d'un écoulement laminaire entièrement établi dans un tuyau courbe donne un résultat satisfaisant pour le coefficient de perte de charge et le coefficient de transport de chaleur dans un champ de température entièrement établi sous la condition de flux de chaleur uniforme à de grands nombres de Dean $[=Re\sqrt{(a/R)}]$. Le rapport du nombre de Nusselt pour un écoulement dans un tube courbe à celui pour l'écoulement dans un tube rectiligne est obtenu en fonction du nombre de Dean et du nombre de Prandtl. Lorsque le nombre de Prandtl et le nombre de Dean augmentent, l'effet de la courbure sur la perte de charge et le transport de chaleur croît, mais le rapport des nombres de Nusselt approche de la valeur asymptotique lorsque le nombre de Prandtl croît. Une étude expérimentale a été conduite pour l'écoulement de l'air dans un tuyau courbe. Les distributions de vitesse et de température sont mesurées et on montre que le rapport des nombres de Nusselt obtenu par l'expérience est en bon accord avec celui obtenu par l'analyse théorique.

Zusammenfassung—Die theoretische Untersuchung einer voll ausgebildeten laminaren Strömung in einem gekrümmten Rohr gibt für den Widerstandsbeiwert und die Wärmeübergangszahl in einem völlig ausgebildeten Temperaturfeld unter der Bedingung einer gleichförmigen Wärmestromdichte bei grossen Dean-Zahlen $[=Re\sqrt{(a/R)}]$ ein zufriedenstellendes Ergebnis. Wird die Nusselt-Zahl für die Strömung im gekrümmten Rohr zu der Nusselt-Zahl für die Strömung in geraden Rohr ins Verhältnis gesetzt, so ist dieses Verhältnis eine Funktion der Dean- und der Prandtl-Zahl. Wenn diese beiden Zahlen grösser werden, steigt auch der Einfluss der Krümmung auf den Strömungswiderstand und den Wärmeübergang. Das Verhaltnis der Nusselt-Zahlen nähert sich jedoch bei wachsender Prandtl-Zahl dem Grenzwert. Experimentelle Untersuchungen wurden an einem luftdurchströmten, gekrümmten Rohr ausgeführt. Geschwindigkeits- und Temperaturverteilung werden gemessen und für das experimentell bestimmte Verhältnis der Nusselt-Zahlen ergibt sich eine gute Übereinstimmung mit den theoretisch ermittelten Werten.

Аннотация—Теоретическое изучение полностью развитого ламинарного течения в изогнутой трубе дает удовлетворительные результаты для коэффициентов сопротивления и теплообмена при полностью сформировавшемся температурном поле и в условиях одинакового теплового потока при больших числах Дина $[=Re\sqrt{(a/R)}]$. Отношение числа Нуссельта для потока в изогнутой трубе к числу Нуссельта для потока в прямой трубе получено в виде функции числа Дина и числа Прандтля. При увеличении чисел Дина и Прандтля влияние кривизны на сопротивление потока и теплообмен увеличивается, соотношение чисел Нуссельта достигает асимптотического значения при увеличивающемся значении числа Прандтля. Проводилось экспериментальное изучение потока воздуха в изогнутой трубе. Измерялись распределения скорости и температуры. Показано, что экспериментально полученное соотношение чисел Нуссельта хорошо согласуется с теоретическим.